A Wavenumber-Frequency Analysis of the 500 mb Geopotential at 50°N

KLAUS FRAEDRICH AND HORST BÖTTGER

Institut für Meteorologie, Freie Universität Berlin, Berlin, West Germany

8 August 1977 and 19 December 1977

ABSTRACT

A space-time spectral analysis is applied to the daily 500 mb geopotential field (gridded along 50°N) of five winter seasons (1972–77). The results are displayed in the wavenumber-frequency domain as two-sided frequency spectra of meridional geostrophic wind and one-sided spectra of geopotential. They show three isolated spectral peaks: stationary ultralong waves ($k=1$–4, $p\approx 25$ days), and eastward propagating long ($k=5$–6, $p\approx 10$ days, $c\approx 6$ m s^{-1}) and short waves ($k=7$–8, $p=4$–6 days, $c\approx 10$ m s^{-1}). In the wavenumber-frequency domain only the magnitudes of the peaks vary from one season to the other.

1. Introduction

Some interesting features appear in a comprehensive space-time spectral analysis which has been applied to the mid-latitudes of a Northern Hemispheric winter general circulation experiment (Hayashi and Golder, 1977; Gall, 1976). For instance, three isolated spectral peaks of the variance density of the meridional wind, for example, can be identified in the wavenumber-frequency domain: stationary ultralong waves (latitudinal wavenumber $k=1$–3, period $p\approx 30$ days), propagating long waves (wavenumber $k=5$, period $p=12$ days, speed $c=6$ m s^{-1}) and propagating short waves (wavenumber $k=7$, period $p=4$–6 days, speed $c=12$ s^{-1}). But, observed data have not been presented to corroborate this finding, especially the appearance of the isolated peak of the long propagating waves. This, however, may be due to the fact that there exist only a few investigations from which such a spectral separation can be inferred. Kao and Wendell's (1970) spectra, these do not warrant such specific conclusions; other papers (e.g., Willson, 1975) are mainly concerned with the spectral structure (power laws, cutoff frequency or wavenumber, etc.) and their season and latitude dependent behavior.

Therefore, it is the purpose of this note to present observational evidence of the three isolated spectral peaks in the wavenumber-frequency domain; viz., the two main types of the propagating long and short waves corresponding to larger and smaller cyclones, and the stationary ultralong wave phenomena which are thermally and orographically forced.

2. Method and data

Fourier analysis provides a method to transform data of the space-time domain into the wavenumber-frequency space (Kao, 1968). A modification of this technique is the space-time spectral analysis of atmospheric or model-output data, for example, which more properly treats the stochastic nature of the time series (Hayashi, 1971). Both analyses specify the variance densities contributed by the eastward or westward propagating waves. The background for the interpretation of both methods, including their differences, shortcomings, etc., is described by Pratt (1976), whose notation is adopted.

In this paper the space-time *spectral analysis* is applied, for which two-sided (Hayashi, 1971) and one-sided (Pratt, 1976) frequency spectra can be defined.

1) The *two-sided* frequency spectrum E at a wavenumber k defines the components of eastward ($+\omega$) and westward ($-\omega$) propagating waves for a frequency band centered at ω:

$$E(k,\pm\omega)=\tfrac{1}{4}\{P_\omega(C_k)+P_\omega(S_k)\}\pm\tfrac{1}{2}Q_\omega(C_k,S_k). \quad (2.1)$$

Here P_ω and Q_ω are the power and quadrature spectral densities of the longitude λ and time t dependent function $q(\lambda,t)$ expanded in zonal Fourier harmonics:

$$q(\lambda,t)=q_0(\lambda,t)+\sum_{k=1}^{\infty}\{C_k(t)\cos k\lambda+S_k(t)\sin k\lambda\}.$$

2) The *one-sided* (total) space-time variance density spectrum $T(k,\omega)$ is given by the sum of the eastward and westward propagating contributions of (2.1):

$$T(k,\omega)=\tfrac{1}{2}\{P_\omega(C_k)+P_\omega(S_k)\}. \quad (2.2)$$

The *propagating* variance density spectrum $PR(k,\omega)$ is defined by the difference of the eastward and westward contributions of (2.1):

$$PR(k,\omega)=|Q_\omega(C_k,S_k)|. \quad (2.3)$$

The propagation direction can be inferred from the sign of Q_ω. The *stationary* variance density spectrum

$$SR(k,\omega)=T(k,\omega)-|Q_\omega(C_k,S_k)| \quad (2.4)$$

0022-4928/78/0745-0750$05.00

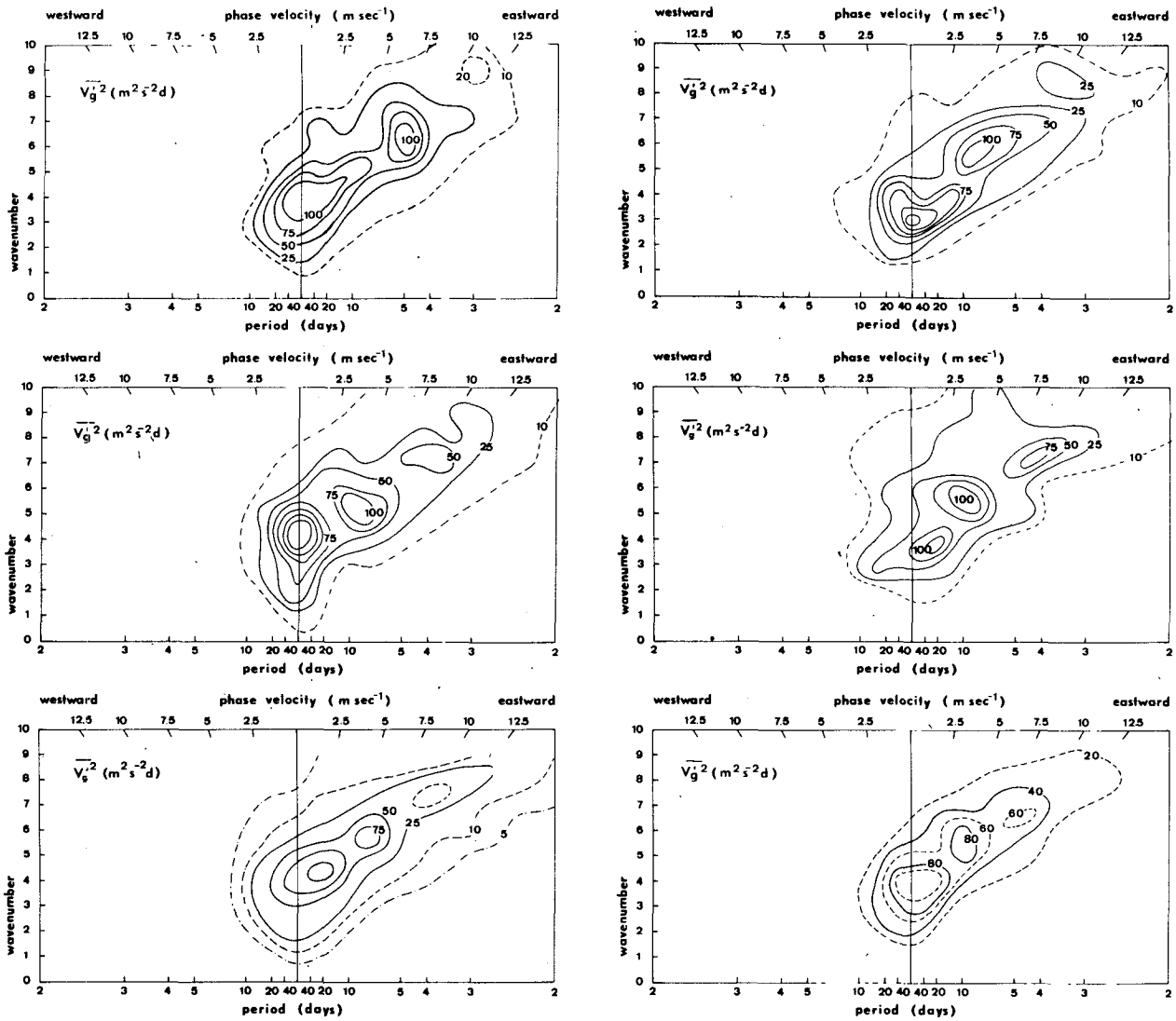

FIG. 1. Power spectrum density of the meridional geostrophic wind at 500 mb and 50°N (two-sided frequency spectrum). Upper left to middle right: winter 1972/73 to 1976/77, and the average (lower right).

includes all nonpropagating waves fluctuating in time (Hayashi, 1977). They may reflect a mixture of true stationary and random fluctuations. To avoid the contribution of the random fluctuations to the stationary spectrum, one may use a formulation suggested by Pratt [1976, Eq. (12)] replacing (2.4).

In addition, the longitudinal phase $\phi(k,\omega)$ of the antinode of the stationary oscillation can be determined from

$$\phi(k,\omega)=\arctan\left[\frac{2K_\omega(C_k,S_k)}{P_\omega(C_k)-P_\omega(S_k)}\right],$$

where K_ω is the cospectrum.

Spectral analysis is applied to daily geopotential height values z for the five winter seasons from 1972/73 to 1976/77, which start at the first of November and last for 120 days. A set of seasons is investigated in order to qualitatively judge the confidence of conclusions to be drawn from finite sample statistics and to show the variability. The data are obtained from subjectively drawn 500 mb pressure level analyses on a 10° grid around the 50°N latitude circle (~25 000 km). The Fourier harmonics are cut off at wavenumber $k=10$ beyond which the remaining zonal variance appeared to be negligibly small (<5%). A lag correlation method with a 20-day lag was used. To obtain smooth spectral estimators, the Tukey lag window was applied with an equivalent bandwidth $b=b_1$/maximum lag. The standardized bandwidth of the Tukey window $b_1\doteq 4/3$ gives $b=1/15$ cpd with 16 degrees of freedom (see, e.g., Jenkins and Watts, 1969). Low-frequency variances were not removed because the data did not show any trend.

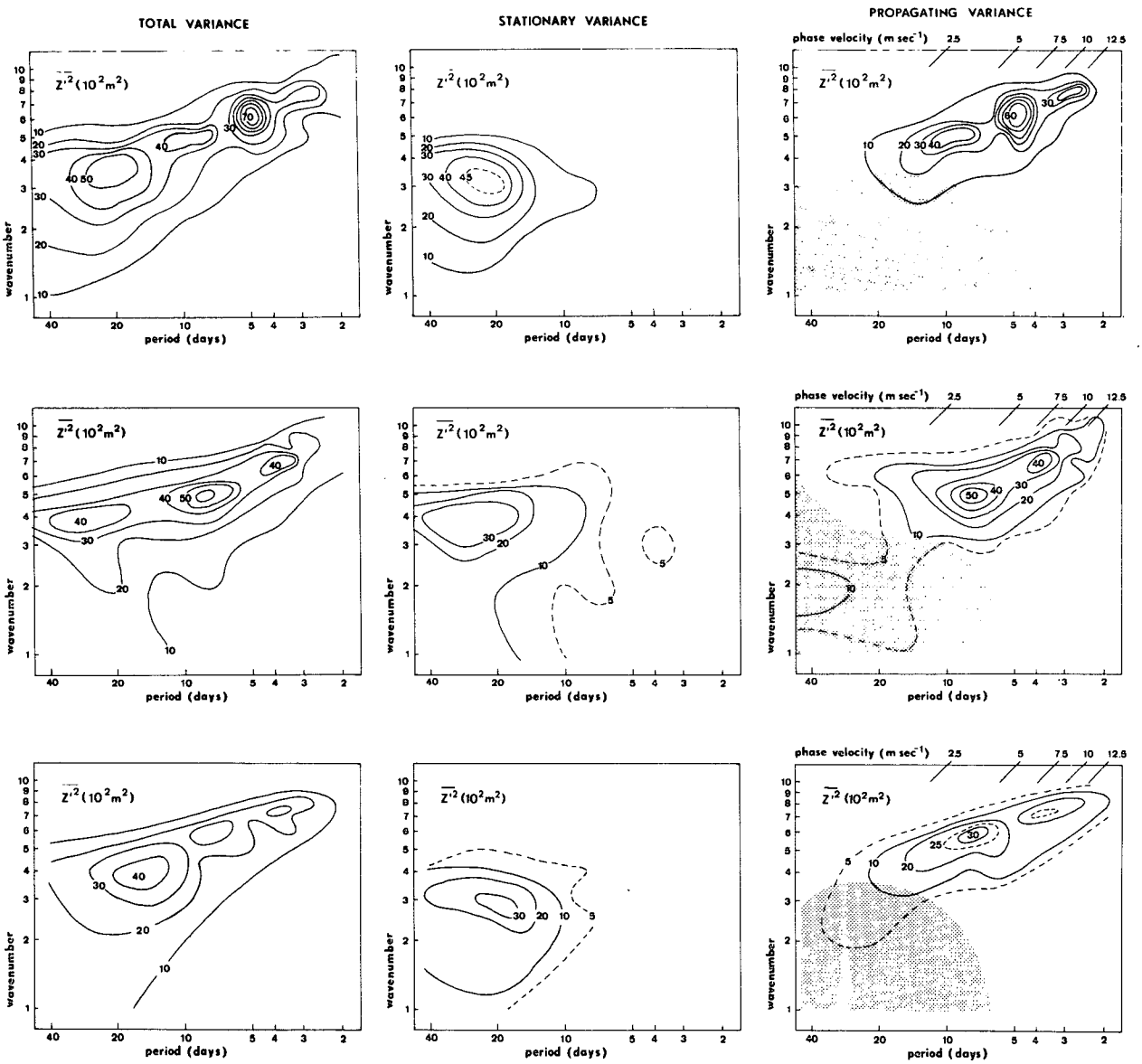

FIG. 2. Power spectrum of geopotential at 500 mb and 50°N (one-sided frequency spectrum). From top to bottom: winter 1972/73 to 1974/75. Shaded area: westward propagation.

3. Results

The result of the spectral analysis is presented in two ways:

1) The two-sided frequency spectra (2.1) are displayed for the geostrophic meridional wind v_g in a linear wavenumber-frequency diagram [comparable to that used by Hayashi and Golder (1977)]. The values are simply derived from the z spectra by multiplication with $g^2k^2/(a^2f^2\cos^2\varphi)$ with the earth's acceleration g, its radius a and the Coriolis parameter f at latitude $\varphi=50°$N (Fig. 1).

2) The one-sided frequency spectra [(2.2)–(2.4)] for the geopotential height z are displayed in a double-logarithmic presentation of the wavenumber-frequency dependent variance density (multiplied by wavenumber k and frequency ω). As the spatial variance is distributed over a series of discrete lines in k the total variance in a cut $\Delta\omega$ is obtained when summed over k. Therefore, the exact positions of the spectral peaks in the contour fields drawn subjectively should be interpreted according to the restriction mentioned above.

Both presentations, of course, show the same structures. They appear more obvious if one-sided spectral distributions are considered, because the variances are separated into propagating and stationary contribu-

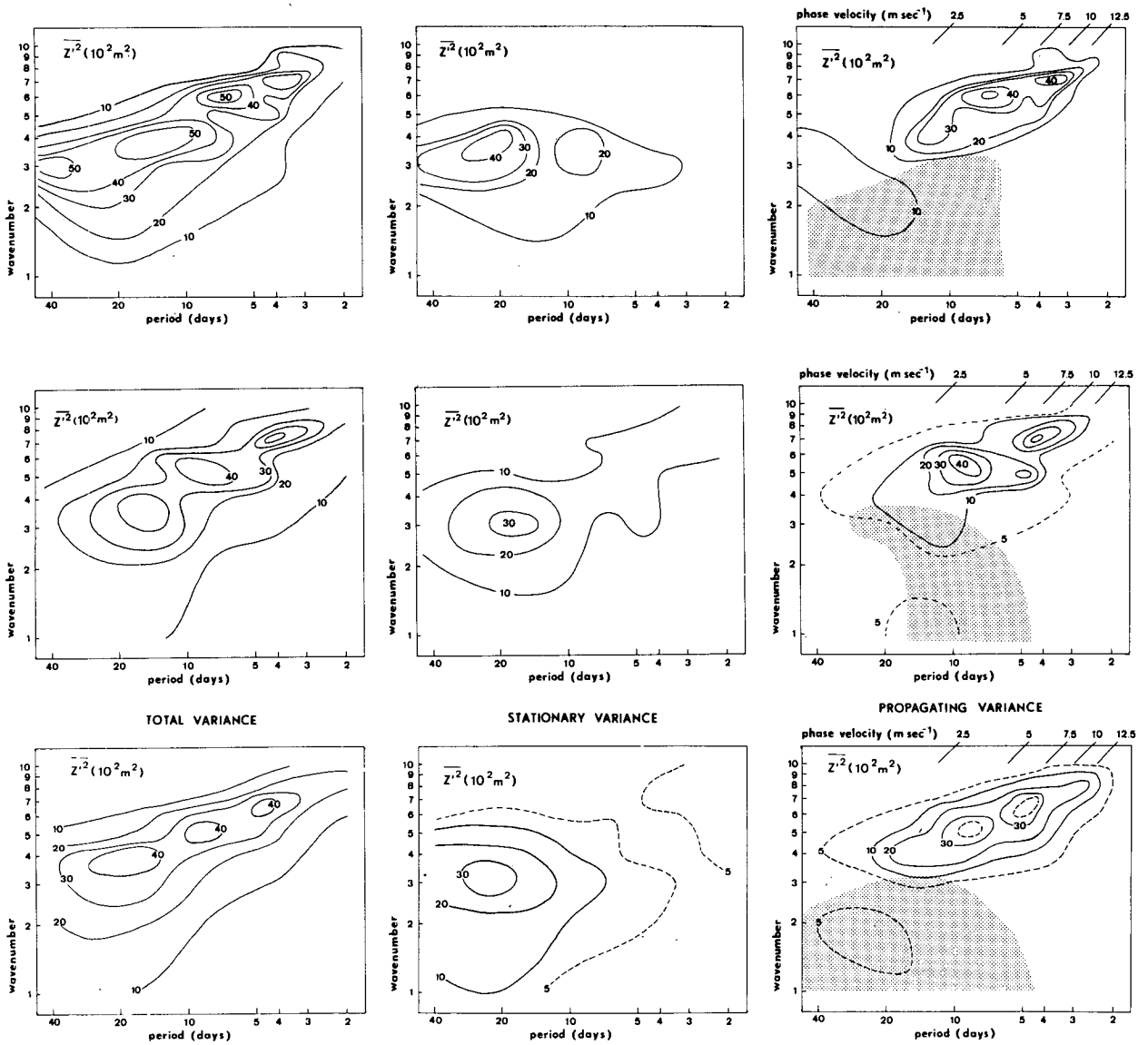

FIG. 2. *Continued.* [Top to bottom, winter 1975/76, 1976/77 and average.]

tions to the total. For the two-sided frequency spectra, however, both contributions are jointly displayed.

The observational results are in general agreement with those of Hayashi and Golder (1977) suggesting the presence of three distinct maxima of variance. For a direct comparison it should be realized that the model spectra are determined for the actual 300 mb meridional wind, whereas ours refer to the 500 mb meridional geostrophic wind component. Three spectral peaks can be identified during almost all winter seasons in Fig. 1. Differences in the propagating variance density are mainly due to the variability of their magnitudes, but there always seem to be two maxima. The maxima of the stationary variance show no significant variation on position, and have values which vary about wavenumbers 3 and 4 and periods of 25 days (Fig. 2).

Consequently, the average spectral variance densities of the five winter seasons are not smoothed out but clearly exhibit three spectral peaks in Fig. 1: the eastward propagating long waves ($k=5$–6, $p=8$–10 days, $c=6$ m s^{-1}) and short waves ($k=7$–8, $p=4$–6 days, $c\approx 10$ m s^{-1}), and the stationary ultralong waves ($k=1$–4, $p\approx 20$–30 days).

Direct synoptic evidence for the existence of these spectral peaks can be gained from a Hovmöller diagram for the winter season 1976/77 (Fig. 3). Geopotential heights of the 500 mb level at 50°N are plotted daily from 180°W to 170°E commencing on 1 November. The oscillation of the stationary ultralong waves is quite obvious over the eastern Pacific and North America and over the Atlantic and Europe. Two main types of traveling waves are traced by following the minima of geopotential height. Their slopes are a

measure of the phase speeds of the traveling waves. At a fixed longitude these waves occur at periods indicated by the consecutive distance of the sloping lines, different for short and long traveling waves. First, propagating long waves of phase speed $c \approx 6$ m s^{-1} and period $p \approx 10$ day (full line) correspond to wavenumber $k = 5$–6; second, short waves of phase speed $c \approx 10$ m s^{-1}, period $p \approx 4$–6 days (dashed line) correspond to wavenumber $k = 7$–8. In Fig. 3 these waves are only marked in those areas where they can be found objectively (as defined above). Still the picture is in good agreement with the results of the cross-spectral analysis.

The spectra of total variance were tested against first-order Markov process spectra of the same total variance. The three peaks of the 500 mb geopotential spectra for one season (winter 1976/77) exceed the red noise spectra by factors of 2.0–2.6, corresponding to an *a priori* confidence of 95% or more when compared to a chi-square distribution with 16 degrees of freedom.

The three averaged peaks of the one-sided total variance spectrum (Fig. 2) vary according to $f \propto k^4$

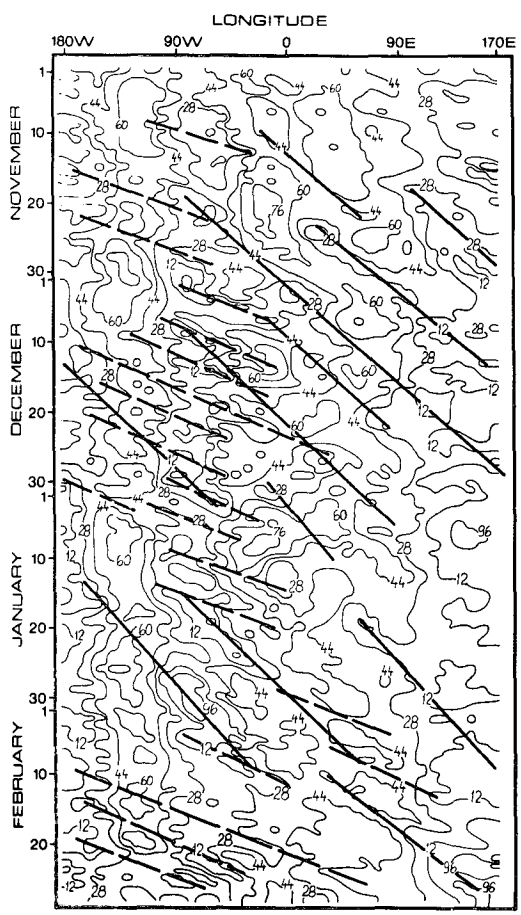

FIG. 3. Time-longitude (Hovmöller) diagram of 500 mb geopotential (units, geopotential dam) for winter 1976/77 at 50°N. Full (dashed) lines indicate long (short) traveling troughs.

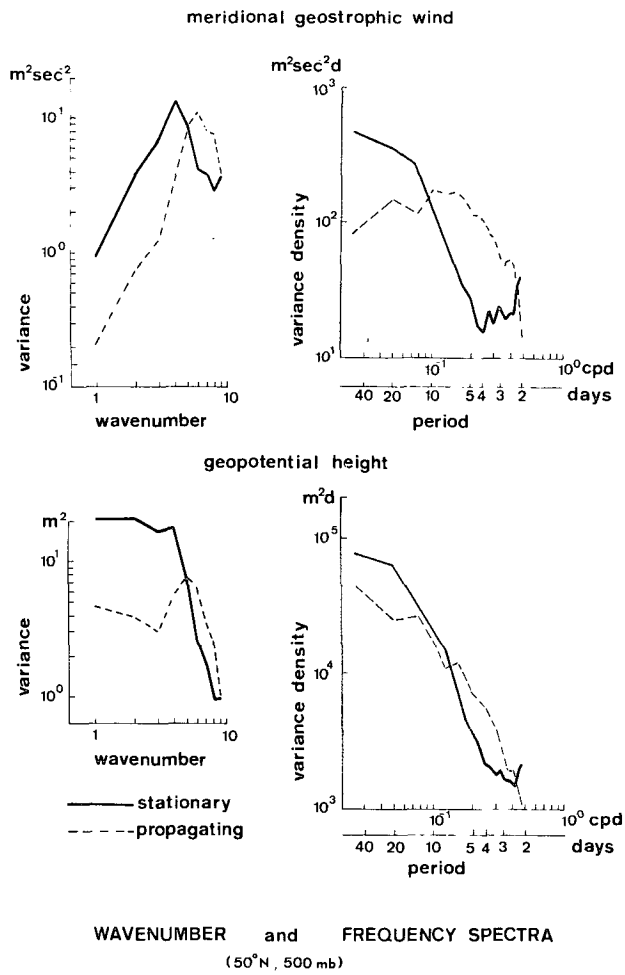

FIG. 4. Wavenumber and frequency integrated spectra of geostrophic wind v_g and geopotential z.

(frequency $f = \omega/2\pi$). The averaged variance densities fall off sharply at both sides of this peak variation as is evident from the frequency- or wavenumber-integrated variance densities. Above a cutoff frequency or wavenumber these slopes may be described by power laws which are determined for stationary and propagating variance densities (Fig. 4):

1) After integrating the variance densities over frequency one obtains the slopes toward higher wavenumbers k (Fig. 4), where the parts of the propagating (PR) and stationary (SR) variances can be separated:

$$\int PR\,df \propto k^{-(4 \text{ to } 5)}, \quad \int SR\,df \propto k^{-(3 \text{ to } 4)}.$$

2) After integrating the variance densities over wavenumber, the slopes toward higher frequencies yield (Fig. 4)

$$\int PR\,dk \propto f^{-(2 \text{ to } 3)}, \quad \int SR\,dk \propto f^{-(1 \text{ to } 2)}.$$

4. Conclusion

Some observational evidence is presented to show the existence of three spectral peaks of the geopotential (meridional geostrophic wind) variance appearing in the wavenumber-frequency domain. The two spectral peaks of propagating variance may simply be explained by the two types of baroclinic instability which favor two distinct wavelengths for processes characterized by a static stability of dry and moist saturated air (Mintz, 1961; see also Fortak, 1971); however, a more complex interpretation by Gall (1976) may be preferred. The peaks in the stationary variance density spectrum at periods of ~25 days can be identified with the vacillation as described by Namias (1950), McGuirk and Reiter (1976) and Webster and Keller (1975). Moreover, a strong annual variability can also be inferred from these figures, for which they provide a quantitative measure.

Acknowledgments. Thanks are due to Dr. Y. Hayashi and other referees for valuable comments, to Ms. C. Kirsch, and E. Neumann for preparing the data, Ms. M. Lungwitz, and U. Eckertz-Popp, and Mr. H. Haug for typing, photographing and drafting.

REFERENCES

Gall, R., 1976: A comparison of linear baroclinic instability theory with the eddy statistic of a general circulation model. *J. Atmos. Sci.*, **33**, 349–373.

Fortak, H., 1971: *Meteorologie.* Carl Habel, Verlag, 287 pp.

Hayashi, Y., 1971: A generalized method of resolving disturbances into progressive and retrogressive waves by space Fourier and time cross-spectral analysis. *J. Meteor. Soc. Japan*, **49**, 125–128.

——, 1977: On the coherence between progressive and retrogressive waves and a partition of space-time power spectra into standing and traveling parts. *J. Appl. Meteor.*, **16**, 368–373.

——, and D. G. Golder, 1977: Space-time spectral analysis of mid-latitude disturbances appearing in a GFDL general circulation model. *J. Atmos. Sci.*, **34**, 237–262.

Jenkins, S. M., and D. G. Watts, 1969: *Spectral Analysis and Its Applications.* Holden-Day, 525 pp.

Kao, S.-K., 1968: Governing equations and spectra for atmospheric motion and transports in frequency-wavenumber space. *J. Atmos. Sci.*, **25**, 32–38.

——, and L. L. Wendell, 1970: The kinetic energy of the large-scale atmospheric motion in wavenumber-frequency space: I. Northern Hemisphere. *J. Atmos. Sci.*, **27**, 359–375.

McGuirck, J. P., and E. R. Reiter, 1976: A vacillation in atmospheric energy parameters. *J. Atmos. Sci.*, **33**, 2079–2093.

Mintz, Y., 1961: The general circulation of planetary atmospheres. Nat. Res. Council Publ. 944, Washington, D.C., 107–146.

Namias, J., 1950: The index cycle and its role in the general circulation. *J. Meteor.*, **7**, 130–139.

Pratt, R. W., 1976: The interpretation of space-time spectral quantities. *J. Atmos. Sci.*, **33**, 1060–1066.

Webster, P. J., and J. L. Keller, 1975: Atmospheric variations: Vacillation and index cycles. *J. Atmos. Sci.*, **32**, 1283–1300.

Willson, M. A. G., 1975: A wavenumber-frequency analysis of large-scale tropospheric motions in the extratropical Northern Hemisphere. *J. Atmos. Sci.*, **32**, 478–488.